Robotica (2008) volume 26, pp. 635–641. © 2008 Cambridge University Press
doi:10.1017/S0263574708004244 Printed in the United Kingdom

Dynamic analysis of AGV control under dead-reckoning algorithm

Abílio Azenha[1,*] and Adriano Carvalho[2]

Institute for Systems and Robotics, Faculty of Engineering, University of Porto,
Rua Dr. Roberto Frias s/n, 4200–465 Porto, Portugal

(Received in Final Form: February 6, 2008. First published online: March 19, 2008)

SUMMARY

In this paper, dead-reckoning localization errors for automated guided vehicles (AGVs) in indoors quasi-structured environments are studied. Based on error ellipse localization analysis, dead-reckoning errors arising from mismatched AGV wheels radius are investigated. The dynamic model for a differential-drive AGV type with mismatched wheels radius is also derived. The developed rationale shows that sensor fusion is a key feature for minimizing AGV localization errors. Two simulation scenarios and one experiment are presented to show system performance under AGV proportional-derivative (PD)-type control.

KEYWORDS: AGV control; Dead-reckoning; Measurement error analysis; Localization; Simulation.

1. Introduction

Automated guided vehicle (AGV) control[1,2] is prone to systematical, non-systematical, and numerical drift errors;[3–5] and AGV navigation in indoors environments cannot resort to global positioning system (GPS)[6] because GPS signals are weakened by the building structure. In industry, AGVs are adopted in automatic warehouses and in handling materials equipment. In general, AGV control is composed of two stages: low accuracy and high accuracy positioning requirements. Low accuracy positioning is sufficient in the materials transportation stage and, in the parking stage, high accuracy positioning is required to accomplish transfer of materials. In the materials transportation stage, dead-reckoning with triangulation algorithms[4] can be adopted, because positioning accuracy requirements are not very demanding. In parking stages, other higher accuracy positioning methodologies must be adopted such as ultrasonic sensing.[7] This paper contributes to efficient AGV control and instrumentation needs for autonomous navigation in indoors quasi-structured environments.

By means of dead-reckoning[7,8] (from sailing: deduced reckoning), AGV localization can be carried out with odometry and heading (or orientation) sensing instrumentation components.[5,9–11] As dead-reckoning errors are commonly dependent on travelled distance,[4] some techniques of localization error elimination should be developed, as for example, triangulation procedures.[12] In this paper, the localization needs for efficient control of AGVs are analysed through systematical errors studies, namely, those arising from mismatched AGV wheels radius.

Continuous and discrete system simulation can be done through software packages or *ad hoc* computer programs written in scientific programming languages. Ordinary differential equations can be solved by Runge–Kutta 4 algorithm, which can have good performance. Continuous system parts can be simulated at sampling frequencies of some 100 kHz and discrete system parts at a much lower sampling frequency, as for example 10 Hz. Nowadays, computing power of micro-computers is huge, so complex systems simulation becomes possible and efficient. Having the availability of good computing system models, simulation validates control algorithms and their tuning (e.g. controller parameters and sampling frequency). Numerical simulation makes possible testing systems with much less financial effort than if it should be necessary to build the full physical system.

This paper presents simulation and experimental results of proportional-derivative (PD)-type control of differential-drive AGV models having mismatched wheels radius. Experimental result shows other sources of errors together with systematical errors under dead-reckoning algorithm. The remaining of this paper is organized as follows. Section 2 describes error modelling for mismatched AGV wheels radius, Section 3 derives AGV dynamic model, Section 4 summarizes sensor fusion in dead-reckoning algorithm, Section 5 presents system simulations and an experiment, and ultimately Section 6 draws the main concluding remarks.

2. Error Modelling

Dead-reckoning algorithm is very efficient using AGV internal instrumentation signals for autonomous navigation. Its systematical errors are most likely to induce positioning errors. In the work of Borenstein,[3] two differential-drive mobile robots are physically connected through a compliant-linkage and using one linear and two rotary encoders provided signals adopted by an internal auto-correcting dead-reckoning algorithm. An AGV control scheme for indoors positioning was presented in Azenha *et al.*[13] In this paper, the AGV shown in Fig. 1 is chosen.

* Corresponding author. E-mail: azenha@fe.up.pt

[1] Doctor of Electrical and Computer Engineering, Researcher, Corresponding author.
[2] Doctor of Electrical and Computer Engineering, Senior Researcher.

https://doi.org/10.1017/S0263574708004244 Published online by Cambridge University Press

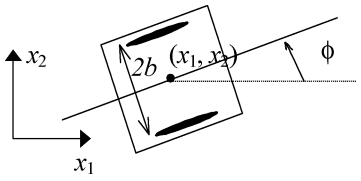


Fig. 1. Adopted AGV model.

The kinematic relationships for this type of AGV are (1), which state the dead-reckoning algorithm

$$\begin{bmatrix} x_{1odom} \\ x_{2odom} \\ \phi_{odom} \end{bmatrix} = \begin{bmatrix} x_{10} + R\cos(\phi_0)(\Delta\theta_1 + \Delta\theta_2)/2 \\ x_{20} + R\sin(\phi_0)(\Delta\theta_1 + \Delta\theta_2)/2 \\ \phi_0 + \dfrac{R}{2b}(\Delta\theta_1 - \Delta\theta_2) \end{bmatrix} \quad (1)$$

where $(x_{1odom}, x_{2odom}, \phi_{odom})$ is the current AGV pose and (x_{10}, x_{20}, ϕ_0) is the previous time-step AGV pose. Angles θ_i $(i = 1, 2)$ are the wheel i angular position, parameter R is the drive wheel radius and b is as shown in Fig. 1. The AGV pose is defined as the position (x_1, x_2) and heading or orientation (ϕ) in the Cartesian space. Figure 2 depicts the current heading (ϕ) and the target heading (ϕ_t) and (x_{1r}, x_{2r}) is the reference AGV position in the Cartesian space.

This paper deals with studying the contribution of dead-reckoning systematical induced errors to the final estimated localization error. It is shown that a good heading measurement accuracy contributes strongly to make triangulation more efficient for a differential-drive AGV model, keeping on quality of measurement. Once the order of magnitude for the localization error is estimated, then the need for performing the triangulation task[12] is therefore evaluated and quantitatively studied. In the following text, the quantitative evaluation of dead-reckoning systematical errors for the AGV type of Fig. 1 is performed.

The two AGV wheels have non-equal radius due to mechanical imperfections, mechanical tolerance, or wheels wearage so radius R_i is assumed to wheel i $(i = 1, 2)$. This source of systematical errors is assumed to be the only one corresponding to dead-reckoning. Heading measurement errors, slips of wheels and uncertainty in other AGV kinematic parameters are not analysed in this paper. A study of dead-reckoning errors of robots caused by noise in the direct reading of wheels speeds can be found in Zhou and Chirikjian.[14]

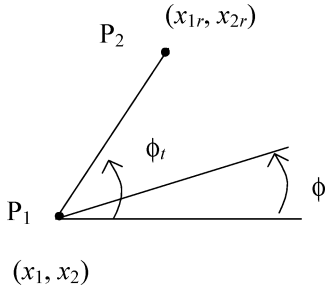


Fig. 2. AGV headings model.

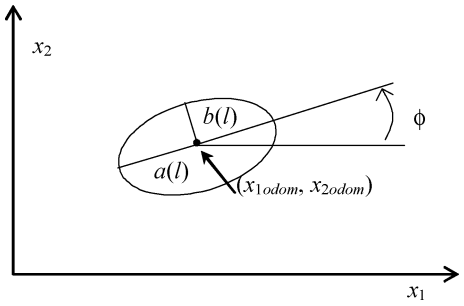


Fig. 3. Error ellipse.

With non-equal wheels radius, the dead-reckoning algorithm can then be derived to (2).

$$\begin{bmatrix} x_1 \\ x_2 \\ \phi \end{bmatrix} = \begin{bmatrix} x_{10} + \cos(\phi_0)(R_1\Delta\theta_1 + R_2\Delta\theta_2)/2 \\ x_{20} + \sin(\phi_0)(R_1\Delta\theta_1 + R_2\Delta\theta_2)/2 \\ \phi_0 + \dfrac{1}{2b}(R_1\Delta\theta_1 - R_2\Delta\theta_2) \end{bmatrix} \quad (2)$$

The equation, in workspace coordinates $\Re^2 \times [0,\ 2\pi)$, for localization uncertainty as function of traveled distance is (3),

$$\frac{(x_1\cos\phi + x_2\sin\phi - x_{1odom})^2}{[a(l)]^2} + \frac{(-x_1\sin\phi + x_2\cos\phi - x_{2odom})^2}{[b(l)]^2} = 1 \quad (3)$$

which is the expression for an ellipse (Fig. 3) where $l = \sum \Delta l$, $\Delta l = \sqrt{\Delta x_{1odom}^2 + \Delta x_{2odom}^2}$ is the distance traveled up to the current estimated position (x_{1odom}, x_{2odom}) and the symbol Δ corresponds to the position increment relative to the dead-reckoning sampling time. The ellipse parameters (4a, b) are an estimate of the total dead-reckoning induced error contribution to the AGV location measurement

$$a(l) = \sum \Delta a(l), \Delta a(l) \cong \Delta a(R_1, R_2, \Delta\theta_1, \Delta\theta_2, \phi_e) \quad (4a)$$

$$b(l) = \sum \Delta b(l),\ \Delta b(l) \cong \Delta b(R_1, R_2, \Delta\theta_1, \Delta\theta_2, \phi_e) \quad (4b)$$

and in the following rationale, these expressions will be evaluated (5a–e), where $K_{\Delta a(l)}$, $K_{\Delta b(l)}$ are error constants,

$$\phi = \phi_0 + \frac{1}{2b}(R_1\Delta\theta_1 - R_2\Delta\theta_2) \quad (5a)$$

$$\phi_{odom} = \phi_0 + \frac{R}{2b}(\Delta\theta_1 - \Delta\theta_2) \quad (5b)$$

$$\phi_e = \phi_{odom} - \phi = \frac{1}{2b}[\Delta\theta_1(R - R_1) - \Delta\theta_2(R - R_2)] \quad (5c)$$

$$\begin{aligned} \Delta a(l) = K_{\Delta a(l)}[&R\cos(\phi_{odom})(\Delta\theta_1 + \Delta\theta_2)\cos(\phi) \\ &+ R\sin(\phi_{odom})(\Delta\theta_1 + \Delta\theta_2)\sin(\phi) \\ &- \cos(\phi_{odom})(R_1\Delta\theta_1 + R_2\Delta\theta_2)\cos(\phi) \\ &- \sin(\phi_{odom})(R_1\Delta\theta_1 + R_2\Delta\theta_2)\sin(\phi)] \\ = K_{\Delta a(l)}&\cos(\phi_e)(R\Delta\theta_1 + R\Delta\theta_2 - R_1\Delta\theta_1 \\ &- R_2\Delta\theta_2) \end{aligned} \quad (5d)$$

https://doi.org/10.1017/S0263574708004244 Published online by Cambridge University Press

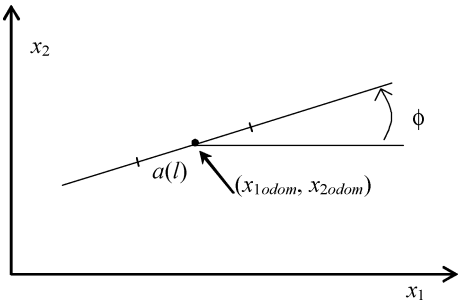


Fig. 4. Error ellipse contribution converted to a line.

$$\begin{aligned}\Delta b(l) = K_{\Delta b(l)}[&-R\cos(\phi_{odom})(\Delta\theta_1+\Delta\theta_2)\sin(\phi)\\ &+R\sin(\phi_{odom})(\Delta\theta_1+\Delta\theta_2)\cos(\phi)\\ &+\cos(\phi_{odom})(R_1\Delta\theta_1+R_2\Delta\theta_2)\sin(\phi)\\ &-\sin(\phi_{odom})(R_1\Delta\theta_1+R_2\Delta\theta_2)\cos(\phi)]\\ =-K_{\Delta b(l)}&\sin(\phi_e)(R\Delta\theta_1+R\Delta\theta_2-R_1\Delta\theta_1\\ &-R_2\Delta\theta_2).\end{aligned} \tag{5e}$$

Analysing Eq. (5e), if $\phi_e = 0$ rad, then $\Delta b(l) = 0$ m and the ellipse becomes a line (Fig. 4). So the line that passes at point (x_{1odom}, x_{2odom}) with slope ϕ is given by Eqs. (6a–b).

$$x_2 - x_{2odom} = \tan(\phi)(x_1 - x_{1odom}) \tag{6a}$$

$$\phi = \pm\frac{\pi}{2} \Rightarrow x_1 = x_{1odom} \tag{6b}$$

Nevertheless, for changing heading angle ϕ, the error ellipse becomes rotated as in (7a, b). The error ellipse contribution becomes a line, but the corresponding overall error ellipse, in general, is not a line:

$$\begin{cases} a_{\Delta\phi}(l) = \Delta a(l) + a(l)\cos(\Delta\phi) + b(l)\sin(\Delta\phi) \\ b_{\Delta\phi}(l) = \Delta b(l) + b(l)\cos(\Delta\phi) - a(l)\sin(\Delta\phi) \end{cases} \tag{7a}$$

$$\Delta\phi = \phi - \phi_0 \tag{7b}$$

where $\Delta\phi$ is the heading angle change and $a_{\Delta\phi}(l)$ and $b_{\Delta\phi}(l)$ are the new error ellipse parameters.

In this context, there is a need for measuring heading angle (ϕ) accurately for reducing AGV location uncertainty. Heading measurement can be done either by a magnetic compass or a MEMS gyroscope. The magnetic compass interferes with other objects, due to the low intensity of Earth magnetic field compared with the noise in some industrial environments, leaving its application almost exclusively to outdoor applications. The MEMS gyroscope has offset and temperature drift errors, which are its main hardware systematical errors; the gyroscope for absolute angle measurement[10,11] eliminates additional time-integration errors that apply to the rate-sensing gyroscope.

3. AGV Dynamic Model

AGV dynamic model[15] is widely known. However, to extend it to the case of mismatched wheels radius, some computations were performed and the adopted AGV dynamic model is (8):

$$\begin{bmatrix}\tau_1\\ \tau_2\end{bmatrix} = \begin{bmatrix} mc_1^2b^2 + Ic_1^2 + I_{w1} & mc_1c_2b^2 - Ic_1c_2 \\ mc_1c_2b^2 - Ic_1c_2 & mc_2^2b^2 + Ic_2^2 + I_{w2}\end{bmatrix}\begin{bmatrix}\ddot{\theta}_1\\ \ddot{\theta}_2\end{bmatrix} + \begin{bmatrix}F_{v1} & 0\\ 0 & F_{v2}\end{bmatrix}\begin{bmatrix}\dot{\theta}_1\\ \dot{\theta}_2\end{bmatrix} \tag{8}$$

where τ_i, F_{vi}, θ_i $(i = 1, 2)$ are the drive dc motors torques, viscous friction coefficients and wheel i angular position, respectively, and:

$$I_C = m_C\frac{4b^2 + l^2}{12} \tag{9a}$$

$$I_{wi} = m_w\frac{R_i^2}{2}, \quad i = 1, 2 \tag{9b}$$

$$I_{mi} = m_w\left(3R_i^2 + t_w^2\right), \quad i = 1, 2 \tag{9c}$$

$$I = I_C + 2m_wb^2 + I_{m1} + I_{m2} \tag{9d}$$

$$m = m_C + 2m_w \tag{9e}$$

$$c_i = \frac{R_i}{2b}, \quad i = 1, 2 \tag{9f}$$

where l is the AGV length, t_w is the transversal wheel length, m_c is the AGV mass without wheels and drive motors and m_w is the wheel with motor mass, R_i $(i = 1, 2)$ are the drive wheels radius and b is as shown in Fig. 1. This model was derived according to the study presented by Yun and Yamamoto[15] and, as it can be verified, significant parameters of the model are dependent on mismatched wheels radius.

4. Sensor Fusion

As presented in Section 2, dead-reckoning AGV navigation algorithm relies on odometry and on heading sensor instrumentation components. In the absence of measurement errors and in the absence of systematical and non-systematical dead-reckoning errors, only the measurement of wheels angular displacements would be sufficient to accurately locate the AGV. By means of odometry only, therefore, AGV localization would be possible.

In the presence of localization errors, heading sensing becomes a fundamental issue. If AGV location measured through odometry is different from AGV location measured through odometry and heading sensing together, then there are measurement errors. So, without heading sensing, Eq. (1) corresponds to available dead-reckoning algorithm. With heading sensing, dead-reckoning algorithm becomes (10):

$$\begin{bmatrix}x_{1odom}\\ x_{2odom}\\ \phi_s\end{bmatrix} = \begin{bmatrix}x_{10} + R\cos(\phi_s)(\Delta\theta_1 + \Delta\theta_2)/2\\ x_{20} + R\sin(\phi_s)(\Delta\theta_1 + \Delta\theta_2)/2\\ \text{current measured heading}\end{bmatrix} \tag{10}$$

Equation (10) eliminates heading measurement error propagation if heading accuracy is sufficient, because, in

https://doi.org/10.1017/S0263574708004244 Published online by Cambridge University Press

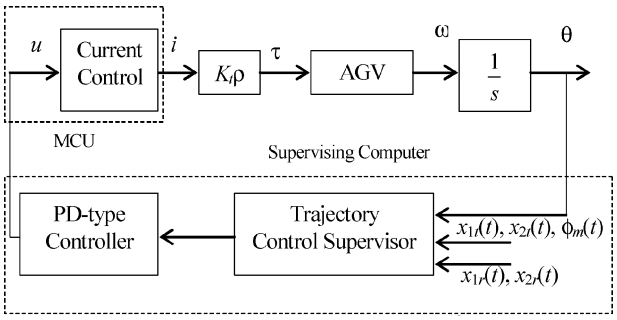


Fig. 5. AGV control scheme.[13]

Eq. (1), ϕ is calculated through wheels angular position measurements. In fact, if Eqs. (1) and (10) are compared, it becomes clear that accurate heading measurement reduces error propagation. In this context, application of sensor fusion guarantees an improvement of localization accuracy.

5. Results

In this section, two simulations and one experimental result are presented to test system performance. Controller performance is tested through simulation and an experiment further demonstrates heading measurement accuracy importance even in the case of strong detrimental errors effects.

5.1. Simulations

This sub-section presents system simulation for a type of PD controller.

The controller attempts to align ϕ with ϕ_t (Fig. 2). In this paper, the controller therefore, relies on dead-reckoning and triangulation schemes. In the work of Azenha *et al.*[13] the localization error was reset by triangulation position and AGV compass/gyroscope heading measurements and their induced errors were neglected, and the control scheme was implemented by the AGV micro-controller (MCU) and by the supervising computer in a way as depicted in Fig. 5. In this figure, (x_{1t}, x_{2t}) and ϕ_m are the AGV position updated by triangulation and orientation updated by internal measurement, respectively. The supervising computer generates the trajectory off-line and handles the communications between the beacons and the AGVs additionally.

Figure 5 parameters are defined as follows: K_t is the current to torque constant and ρ is the gear ratio; i is the dc motor armature current, τ is the wheel input shaft torque and u is the input current control voltage signal.

The PD-type controller (11a–h) is tuned for minimizing trajectory error, taking the system dynamics into account, and it is based on a commercial model,[16] adapted to this system requirements, with sampling time T. The MCU level controls dc motors current (12) with a sampling time equal or lower than T.

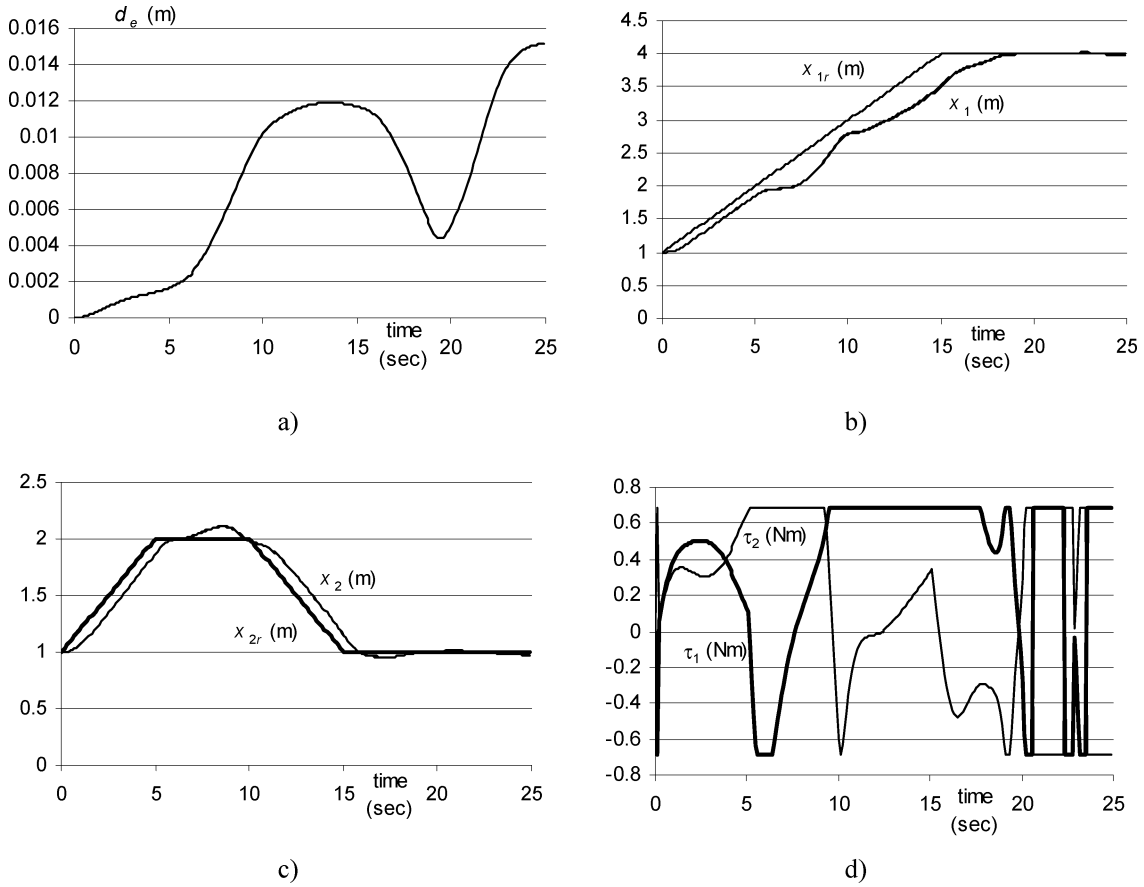


Fig. 6. Simulation results for controller 1: (a) Dead-reckoning distance error (corresponding to mismatched wheels radius only); (b) Trajectory response: reference (x_{1r}) and measured output (x_1); (c) Trajectory response: reference (x_{2r}) and measured output (x_2); (d) Wheels torques.

https://doi.org/10.1017/S0263574708004244 Published online by Cambridge University Press

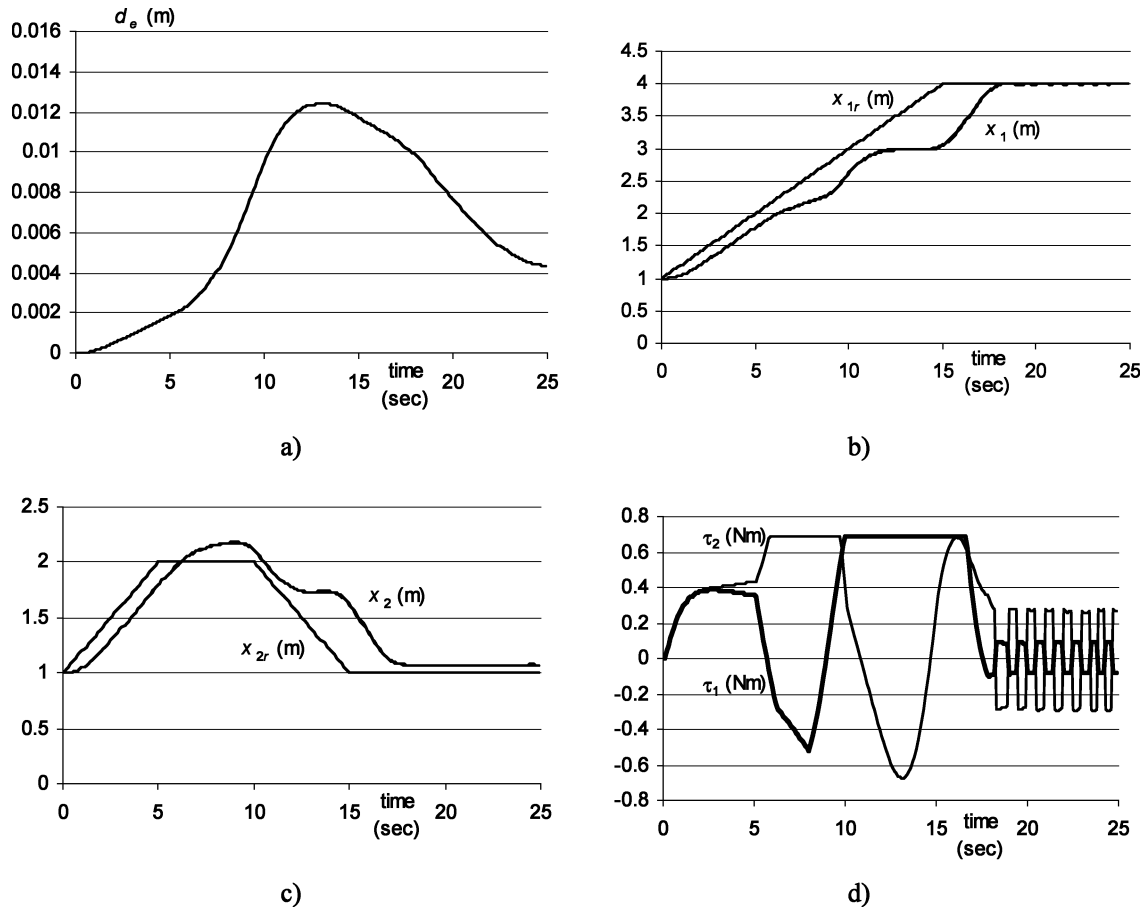


Fig. 7. Simulation results for controller 2: (a) Dead-reckoning distance error (corresponding to mismatched wheels radius only); (b) Trajectory response: reference (x_{1r}) and measured output (x_1); (c) Trajectory response: reference (x_{2r}) and measured output (x_2); (d) Wheels torques.

Controller 1:

$$\mathbf{m}(kT) = [Ke(kT) + d(kT)]\begin{bmatrix}1\\1\end{bmatrix} + \alpha_e(kT) \tag{11a}$$

$$e(kT) = \sqrt{[x_{1r}(kT) - x_1(kT)]^2 + [x_{2r}(kT) - x_2(kT)]^2} \times \operatorname{sgn}\{\cos[\phi_e(kT)]\} \tag{11b}$$

$$d(kT) = \frac{1}{NT + T_d}\langle T_d d[(k-1)T] - T_d K N\{c(kT) - c[(k-1)T]\}\rangle \tag{11c}$$

$$c(kT) = \sqrt{x_1^2(kT) + x_2^2(kT)} \tag{11d}$$

$$\alpha_e(kT) = \begin{bmatrix}\operatorname{sat}[\phi_e(kT), \varepsilon, -K_\phi]\\ \operatorname{sat}[\phi_e(kT), \varepsilon, K_\phi]\end{bmatrix} \tag{11e}$$

$$\phi_e(kT) = \phi_t(kT) - \phi(kT) \tag{11f}$$

$$\operatorname{sat}(a, b, c) = \begin{cases} -c, & a \le -b \\ \dfrac{c}{b}a, & -b < a < b \\ c, & a \ge b \end{cases} \tag{11g}$$

$$\mathbf{u}(kT) = \operatorname{sat}[\mathbf{m}(kT), 5, 5] \tag{11h}$$

$$\mathbf{i} = \frac{1}{10R_S}\mathbf{u} \tag{12}$$

where R_s is the AGV wheels dc motors control bridges current setup resistance.

For comparison, controller 2 was implemented also, with Eq. (13) instead of (11a):

Controller 2:

$$\mathbf{m}(kT) = [Ke(kT) + d(kT)]\left\{\begin{bmatrix}1\\1\end{bmatrix} + \alpha_e(kT)\right\}. \tag{13}$$

The PD-type controller has three error components: a proportional distance, a derivative distance, and a proportional orientation error components. The sum of the three PD-type controller components is the input of the saturation block that models the voltage limitation of the pulse-width modulation dc motors control bridge. In addition, the proportional orientation error component has an output saturation block which enables the stability of this control action, because, in this way, its output is limited in magnitude.

Figures 6 and 7 depict system performance for controllers 1 and 2, respectively. The adopted parameters are: $R_1 = 0.075$ m, $R_2 = 0.069$ m, $R = 0.072$ m, $b = 0.13$ m, $R_S = 1.5\,\Omega$, $m_c = 10$ kg, $m_w = 0.45$ kg, $F_v = 0.1$ Nmsec, $\rho = 66$, $K_t = 0.0311$ Nm/A, $l = 0.4$ m, $t_w = 0.01$ m. AGV

https://doi.org/10.1017/S0263574708004244 Published online by Cambridge University Press

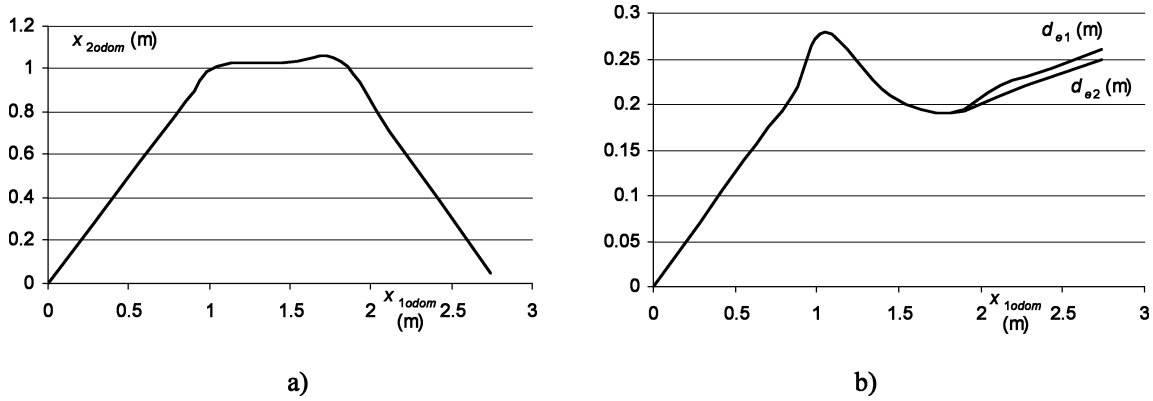


Fig. 8. Experimental result: (a) Dead-reckoning AGV trajectory response: x_{2odom} versus x_{1odom}; (b) Overall dead-reckoning localization distance error without heading sensing (d_{e1}) and with heading sensing (d_{e2}).

system (continuous) sampling simulation frequency was $f_S = 100\,\text{kHz}$ and controller (discrete) sampling simulation frequency was $f_C = 10\,\text{Hz}$. Controller 1 parameters are: $K_\phi = 10\,\text{m}$, $\varepsilon = 0.8\,\text{rad}$, $K = 15$, $T_d = 0.03\,\text{sec}$, $N = 20$. Controller 2 parameters are: $K_\phi = 1.9, \varepsilon = 0.8\,\text{rad}$, $K = 10$, $T_d = 0.03\,\text{sec}$, $N = 20$.

Only mismatched wheels radius systematical errors are considered in the simulations presented.

Simulation results reveal good parking (zeroing of velocities) performance with significant tracking errors due to the controller characteristics. A PD-type controller needs some error to output a signal. As previewed, in general dead-reckoning distance error increases with travelled distance, what points out to analysis performed in Section 2. Output wheels torque should be improved in parking conditions to overcome oscillations.

5.2. *Experiment with wheels slippage*

Figure 8 depicts system performance for an experiment with non-systematical errors,[17] as for example wheels slippage. The adopted AGV parameters are: $R = 7.2 \pm 0.3\,\text{cm}$, $b = 13\,\text{cm}$. A differential-drive AGV type with referred parameters was adopted to perform this experiment.

Figure 8 shows dead-reckoning has localization errors with travelled distance dependency and, even with wheels slippage, heading measurement can somehow improve system performance. Wheels slippage phenomenon has greater influence in the change of direction events, as observed in the experiment. This was significant to test system behavior in the presence of strong detrimental errors effects.

6. Conclusions

This paper describes systematical errors of dead-reckoning navigation algorithm for differential-drive AGVs. Mismatched wheels radius are analysed and the contribution of the localization error on the AGV dynamics is presented. Sensor fusion in dead-reckoning algorithm approaches this issue.

Some results are shown to test the rationale entailed. It is demonstrated that heading sensing improves dead-reckoning algorithm performance even in the presence of strong detrimental errors effects. Mismatched wheels radius for differential-drive AGV types are analysed in the context of their contribution to dead-reckoning algorithm performance. Future work is intended to improve control performance of AGVs taking this study results into consideration.

Acknowledgments

This paper was developed under the grant SFRH/BPD/21033/2004 from Fundação para a Ciência e a Tecnologia (Portugal) and Fundo Social Europeu—III Quadro Comunitário de Apoio (European Union).

References

1. P. Coelho and U. Nunes, "Lie algebra application to mobile robot control: A tutorial," *Robotica* **21**, 483–493 (2003).
2. J.-S. Choi and B. K. Kim, "Near minimum-time direct voltage control algorithms for wheeled mobile robots with current and voltage constraints," *Robotica* **19**, 29–39 (2001).
3. J. Borenstein, "The CLAPPER: A Dual-drive Mobile Robot with Internal Correction of Dead-reckoning Errors," *Proceedings of the IEEE International Conference on Robotics and Automation* San Diego, CA, USA, (1994) pp. 3085–3090.
4. A. Azenha and A. Carvalho, "Indoor Localization Systematical Errors Analysis for AGVs," *13th Saint Petersburg International Conference on Integrated Navigation Systems*, Saint Petersburg, Russia (2006) pp. 199–204.
5. J. M. M. Tur, J. L. Gordillo and C. A. Borja, "A closed-form expression for the uncertainty in odometric position estimate of an autonomous vehicle," *IEEE Trans. Robot.* **21**, 1017–1022 (2005).
6. S.-Y. Yi and B.-W. Choi, "Autonomous navigation of indoor mobile robots using a global ultrasonic system," *Robotica* **22**, 369–374 (2004).
7. J. Borenstein, H. R. Everett and L. Feng, *Navigating Mobile Robots: Systems and Techniques* (A. K. Peters, Wellesley, MA, USA, 1996).
8. D. M. Bevly and B. Parkinson, "Cascaded Kalman filters for accurate estimation of multiple biases, dead-reckoning navigation, and full state feedback control of ground vehicles," *IEEE Trans. Control Syst. Techonol.* **15**, 199–208 (2007).
9. J. Leavitt, A. Sideris and J. E. Bobrow, "High bandwidth tilt measurement using low-cost sensors," *IEEE/ASME Trans. Mechatronics* **11**, 320–327 (2006).
10. D. Piyabongkarn, R. Rajamani and M. Greminger, "The development of a MEMS gyroscope for absolute angle measurement," *IEEE Trans. Control Syst. Technol.* **13**, 185–195 (2005).
11. J. Geen and D. Krakauer, "New iMEMS angular rate-sensing gyroscope," *Analog Dialogue* **37**, 12–15 (2003).

https://doi.org/10.1017/S0263574708004244 Published online by Cambridge University Press

12. A. Azenha and A. Carvalho, "Instrumentation and Localization in Quasi-structured Environments for AGV Positioning," *Preprints of 5th IFAC International Symposium on Intelligent Components and Instruments for Control Applications* Aveiro, Portugal (2003) pp. 73–80.
13. A. Azenha, G. Fernandes and A. Carvalho, "AGV Positioning in Quasi-structured Environments," *11th IEEE International Conference on Methods and Models in Automation and Robotics* Miedzyzdroje, Poland, (2005) pp. 543–548.
14. Y. Zhou and G. S. Chirikjian, "Probabilistic Models of Dead-reckoning Error in Nonholonomic Mobile Robots," *Proceedings of the IEEE International Conference on Robotics and Automation*, Taipei, Taiwan (2003) pp. 1594–1599.
15. X. Yun and Y. Yamamoto, "Internal Dynamics of a Wheeled Mobile Robot," *Proceedings of the IEEE/RSJ International Conference on Intelligent Robots and Systems*, Yokohama, Japan (1993) pp. 1288–1294.
16. J. L. M. de Carvalho, *Dynamical Systems and Automatic Control* (Prentice-Hall International, London, 1993).
17. L. Ojeda, D. Cruz, G. Reina and J. Borenstein, "Current-based slippage detection and odometry correction for mobile robots and planetary rovers," *IEEE Trans. Robot.* **22**, 366–378 (2006).

https://doi.org/10.1017/S0263574708004244 Published online by Cambridge University Press